Journal of Applied Electrochemistry **31**: 355–361, 2001.

Electrodeposition and characterization of Zn–Ni alloys as sublayers for epoxy coating deposition

J.B. BAJAT[1], M.D. MAKSIMOVIĆ[1], V.B. MIŠKOVIĆ-STANKOVIĆ[1]* and S. ZEC[2]
[1]*Faculty of Technology and Metallurgy, University of Belgrade, Karnegijeva 4, PO Box 3503, 11120 Belgrade, Yugoslavia*
[2]*Institute of Nuclear Science "Vinča" PO Box 522, 11001 Belgrade, Yugoslavia*
*(*author for correspondence, e-mail: vesna@elab.tmf.bg.ac.yu)*

Accepted in revised form 3 October 2000

Key words: corrosion, EIS, electrodeposition, epoxy coating, Zn–Ni alloy

Abstract

The chemical composition and phase structure of Zn–Ni alloys obtained by electrodeposition under various conditions were investigated. The influence of the deposition solution and deposition current density on the composition, phase structure, current efficiency and corrosion properties of Zn–Ni alloys were examined. It was shown that the chemical composition and phase structure affect the anticorrosive properties of Zn–Ni alloys. A Zn–Ni alloy electrodeposited from a chloride solution at 20 mA cm^{-2} exhibited the best corrosion properties, so this alloy was chosen for further examination. Epoxy coatings were formed by cathodic electrodeposition of an epoxy resin on steel and steel modified with a Zn–Ni alloy. From the time dependence of the pore resistance, coating capacitance and relative permittivity of the epoxy coating, the diffusion coefficient of water through the epoxy coating, $D(H_2O)$, and its thermal stability, it was shown that the Zn–Ni sublayer significantly affects the electrochemical and transport properties, as well as the thermal stability of epoxy coatings. On the basis of the experimental results it can be concluded that modification of a steel surface by a Zn–Ni alloy improves the corrosion protection of epoxy coatings.

1. Introduction

Zinc alloy deposition has been of interest recently since these alloys provide better corrosion protection than pure zinc coatings [1, 2]. It is known in particular that the mechanical, physical and electrochemical properties can be improved by alloying zinc with nickel [3–6]. Electrochemically deposited Zn–Ni alloys have greater corrosion stability as compared to thermally obtained Zn–Ni alloys [7].

Zinc–nickel alloys exist in various phases and its structure and morphology [8, 9] also determine the corrosion resistance of a deposit. However, it is well known that surface modification can significantly improve the stability of a polymer/metal system against corrosion [10].

The aim of this work was to modify a steel surface by electrodeposition of the Zn–Ni alloy exhibiting the best corrosion properties and to investigate the corrosion behaviour of the Zn–Ni alloy–epoxy coating protective system. Emphasis was placed on determining the electroplating conditions whereby the Zn–Ni alloy with the best corrosion resistance would be obtained. This alloy was then used as a sublayer for epoxy coating electrodeposition. Thin, non-pigmented epoxy coatings (primers) were electrodeposited in order to investigate the effect of the metal surface on the epoxy coating more accurately.

2. Experimental details

2.1. *Electrodeposition of Zn–Ni alloys*

Zn–Ni alloys were deposited galvanostatically on a steel panel or on a rotating disc electrode from chloride [3] and sulphate [11] baths (Table 1). The employed electrolytes were prepared using p.a. chemicals and double distilled water.

The working electrodes were as follows:

(a) A Pt rotating disc electrode (d = 8 mm, at 2000 rpm), for determining the chemical composition. Prior to each electrodeposition, the Pt disc surface was mechanically polished with a polishing cloth (Buehler Ltd), impregnated with a water suspension of alumina powder (0.3 μm grade) and then rinsed with pure water in an ultrasonic bath.

(b) A Cu rotating disc electrode (d = 6 mm, at 2000 rpm), for X-ray diffraction measurements. Prior to each electrodeposition, the Cu disc surface

Table 1. Plating baths

Solution	j/mA cm^{-2}	t/°C
15 g dm^{-3} ZnO 60 g dm^{-3} $NiCl_2 \cdot 6H_2O$ 250 g dm^{-3} NH_4Cl 20 g dm^{-3} H_3BO_3	5–50	40
28.1 g dm^{-3} $NiSO_4 \cdot 7H_2O$ 28.8 g dm^{-3} $ZnSO_4 \cdot 7H_2O$ 5.4 g dm^{-3} NH_4Cl 12.4 g dm^{-3} H_3BO_3	10–40	25

was pretreated in the same manner as the Pt disc surface, described above.

(c) A steel panel (20 mm × 20 mm × 0.25 mm) for electrochemical impedance and TGA measurements, as well as for measurements of the open circuit potential. The test panels were pretreated by mechanical cleaning (polishing) and then degreased in a saturated solution of sodium hydroxide in ethanol, pickled with a 1:1 hydrochloric acid solution for 30 s and finally rinsed with distilled water.

(d) Steel and steel modified by Zn–Ni alloy rotating disc electrodes (d = 8 mm, at 2000 rpm), for polarization measurements. The steel disc surface was pretreated in the same manner as the steel panel surface, described above.

Alternative counter electrodes were as follows:

(a) A nickel spiral wire, placed parallel to the RDEs at a distance of 1.5 cm.

(b) Platinum panels, placed parallel to the steel panel electrode at a distance of 1.5 cm.

The reference electrode used in all experiments was a saturated calomel electrode (SCE).

2.2. *Chemical composition and phase structure determination*

The chemical composition of the Zn–Ni alloy was determined by atomic absorption using a Perkin–Elmer spectrophotometer (AAS-1100).

The phases present in the deposits and the preferred orientation of the deposits were determined by X-ray diffraction (XRD), using a Simens D500 X-ray diffractometer with CuK_α Ni-filtered radiation. The 2θ range of 20–100° was recorded at the rate of 0.02° 2θ/0.5 s. The crystal planes were identified using powder diffraction file (PDF) data.

2.3. *Electrodeposition of epoxy coatings*

Thin nonpigmented epoxy primers were electrodeposited from an epoxy resin modified by amine and isocyanate onto steel and onto a steel surface previously modified by Zn–Ni alloy, using a constant voltage method (CATOLAC emulsion 543.052, produced by Industrie Vernici Italy under a Pittsburg Paint and Glass (PPG) licence). The resin concentration in the electrodeposition bath was 10 wt % solid dispersion in water at pH 5.7; the temperature was 26 °C and the applied voltage was 250 V [12]. After coating for 3 min, the coatings were rinsed with distilled water and cured for 30 min. The film thickness was 22 ± 1 μm.

2.4. *Electrochemical impedance spectroscopy (EIS)*

For a.c. impedance measurements, the coated samples were exposed to a 3% solution of NaCl in distilled water for 48 days. A three-electrode cell arrangement was used. The working electrode was a coated sample situated in a special Teflon holder. The counter electrode was a platinum mesh with a surface area considerably greater than that of the working electrode. The reference electrode was a saturated calomel electrode (SCE). A.C. impedance data were obtained at the open-circuit potential using a PAR 273 potentiostat and PAR 5301 lock-in amplifier. The impedance measurements were carried out over the frequency range of 100 kHz to 10 mHz using a 5 mV sinusoidal voltage. The impedance spectra were analysed using a suitable fitting procedure [13].

2.5. *Determination of the rate of H_2 evolution reaction*

The rate of hydrogen evolution in the polymer solution on steel and steel modified by Zn–Ni alloy was determined on a rotating disc electrode (rotation of 2000 rpm) using slow sweep voltammetry (sweep rate 0.5 mV s^{-1}). The counter electrode was a platinum spiral wire.

2.6. *Gravimetric liquid sorption measurements*

Gravimetric liquid sorption measurements were performed by weighing samples on an analytical balance following immersion in 3% aqueous NaCl solution at 25 °C. The samples were periodically removed from the electrolyte and weighed. Sorption curves were used to evaluate the diffusion coefficient of water across epoxy coatings electrodeposited on steel and steel modified with Zn–Ni alloy surface.

2.7. *Thermogravimetric analysis*

Thermogravimetric analysis (TGA) was carried out using a Perkin–Elmer TGS-2 instrument. The experiments were performed in a dynamic nitrogen atmosphere (30 ml min^{-1}) at a heating rate of 10 °C min^{-1} over the temperature range 23–600 °C. The thermal stabilities of the epoxy coatings were determined from the TG data.

3. Results and discussion

3.1. *Chemical composition of Zn–Ni alloys and current efficiency*

The influence of the deposition current density on the Ni content in the alloy, as well as on the current efficiency, is illustrated in Figures 1 and 2 for alloys deposited from a

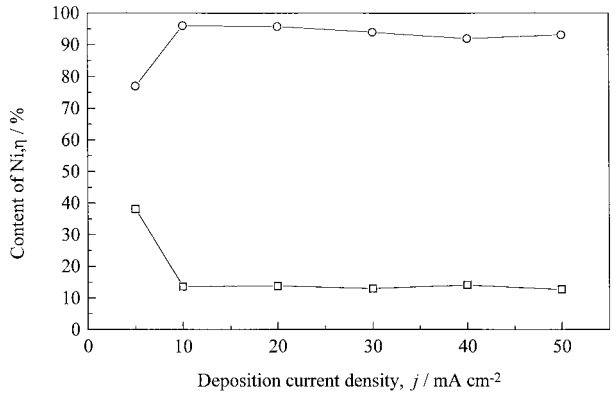

Fig. 1. Dependence of Ni content (□) and current efficiency (○) on deposition current density (alloys were deposited from chloride solution).

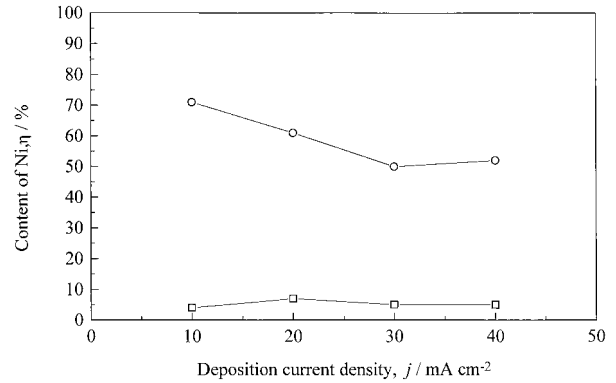

Fig. 2. Dependence of Ni content (□) and current efficiency (○) on deposition current density (alloys were deposited from sulphate solution).

chloride and a sulphate solution, respectively. The overall alloy composition was determined by atomic absorption.

These results are in good agreement with those of Fratesi and coworkers [3] who deposited Zn–Ni alloy from a chloride bath of similar composition and obtained 15–20% of Ni in the alloy. Figures 1 and 2 indicate that electrodeposition from the chloride bath leads to an alloy having a larger content of Ni than the alloy deposited from the sulphate solution, as well as to a deposition with a greater current efficiency. The percentage of Ni remains almost constant regardless of the deposition current density within a broad range of current densities, for both deposition solutions.

Brenner [14] classified the electrodeposition of Zn–Ni alloy as anomalous, where zinc, which is the less noble metal, deposits preferentially. Codeposition of Zn and Ni is however, not always anomalous since, at low current densities, it is possible to obtain normal deposition where Ni deposits preferentially to Zn. Therefore, there is a transitional current density that has to be reached in order to start anomalous codeposition [4].

At low current densities ($j < 10$ A dm^{-2} for deposition from a chloride bath) the Ni content is significantly greater (Figure 1). This increase in the percent of Ni in deposit coincided with a significantly lower current efficiency.

3.2. *Alloy phase structure*

An identification of phase structures present in the Zn–Ni alloys was made on the basis of the chemical composition of the alloys, X-ray diffractograms (XRD) and equilibrium phase diagram of the binary Zn–Ni system [15]. The X-ray diffractograms for Zn–Ni alloys obtained at different current densities and from the two baths are shown in Figure 3(a) and (b). There are three strong and a few weak signals in the case of the Zn–Ni alloy deposited at 20 and 50 mA cm^{-2} from the chloride bath. These deposits consist mainly of γ-phase (Ni_5Zn_{21}) with small amounts of the Zn rich δ-phase (Ni_3Zn_{22}). In the case of the Zn–Ni alloy obtained by 10 mA cm^{-2}, there is a lack of γ-phase with (442, 600) reflections, and the γ-phase (811) and (660) reflections are intensified, relative to the other two deposits.

Besides two strong characteristic γ-phase signals and many weak δ-phase signals, the deposits obtained from the sulphate bath (Figure 3(b)) show additional Zn reflections.

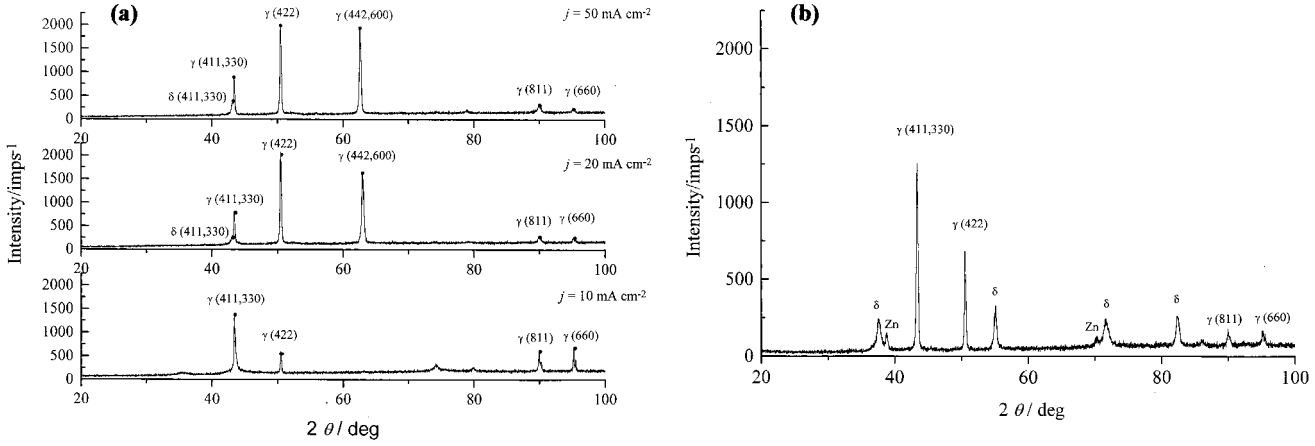

Fig. 3. X-ray diffraction patterns of the Zn–Ni alloys (a) deposited from chloride bath showing the change in the phase distribution and preferred orientation as a function of deposition current density, and (b) deposited from sulphate bath by 30 mA cm^{-2}.

Thus, it has been shown that the type of the plating bath and the nickel content of the alloys have a profound influence on the phase structure of the alloy, whereas the deposition current density has little effect.

3.3. *Corrosion properties of Zn–Ni alloys*

Steel panels were modified by electrodeposition of Zn–Ni alloys at different current densities and the plated specimens were immersed in a 3% aqueous NaCl solution. The open circuit potential (E_{ocp}) was measured daily in order to investigate the corrosion resistance of the Zn–Ni alloys.

The potentials of the Zn–Ni alloys are more negative than that of the steel base, under the same conditions, so Zn–Ni alloys offer sacrificial cathodic protection (Figure 4). The smaller the difference between the potentials of steel and an alloy, the better is the steel protection, the deposit will last longer and the life of the steel base is prolonged.

The E_{ocp} values of steel modified by Zn–Ni alloys increase positively with time of immersion and reach the steel E_{ocp}, which represents loss of the deposit and the start of a corrosion process. The open circuit potentials of alloys deposited at the same current densities from chloride and sulphate baths differ initially but eventually reach almost the same values (Figure 4). The initial E_{ocp} difference is due to the alloy phase difference and the difference in the chemical composition. The Zn–Ni alloy deposited from the sulphate bath is rich in Zn and thus the initial E_{ocp} of this alloy is close to the potential of zinc. The E_{ocp} of Zn–Ni alloy obtained from a chloride bath lies somewhere between the open circuit potentials of pure Zn and pure Ni, since these alloys do not have a Zn-rich phase.

Visually, it could be seen that steel panels with Zn–Ni deposits from the sulphate bath were destroyed first. Of all deposits obtained from the chloride bath, the one deposited by 50 mA cm^{-2} was destroyed first. The alloy deposited from the chloride bath at 20 mA cm^{-2} lasted 2100 h. The results of the visually observed alloy destruction in 3% NaCl solution, or the appearance of the red rust on the steel, are presented in Table 2.

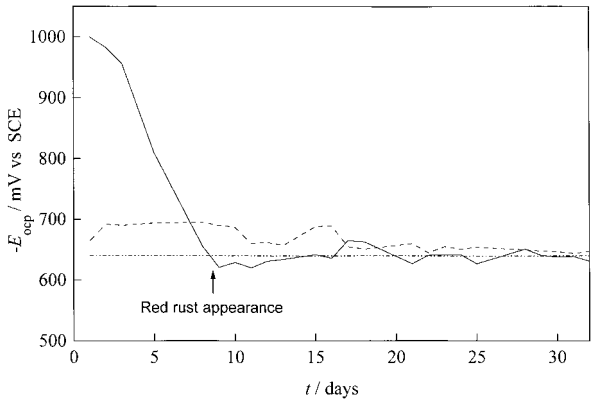

Fig. 4. Time dependence of E_{ocp} for steel modified by Zn–Ni alloys deposited by 20 mA cm^{-2} from chloride and sulfate baths. Key: (- - - - -) steel + Zn–Ni (chloride bath); (——) steel + Zn–Ni (sulfate bath); (– ·· – ·· –) steel.

Table 2. The time of red rust appearance

Type of deposition bath	Deposition current density /mA cm^{-2}	Time/h
Chloride	10	1608
Chloride	20	2100
Chloride	30	696
Chloride	40	504
Chloride	50	384
Sulphate	20	168
Sulphate	50	160

The difference in the corrosion behavior of Zn–Ni alloys deposited from sulphate and chloride baths may be explained on the basis of the chemical composition of the alloy and the phase structure. The reduced protective properties of Zn–Ni alloys obtained from the sulphate bath could be due to the dual δ + Zn phase, which is known to be less resistant to salt corrosion compared to the phases obtained from the chloride bath [4]. Zn–Ni alloys deposited from chloride baths, which have a higher nickel content, consist mostly of γ-phase, which is said to have a higher corrosion resistance [8, 9].

As can be seen from Table 2, the Zn–Ni alloy deposited from a chloride bath at deposition current density of 20 mA cm^{-2} exhibited the best corrosion properties.

This alloy was used for the modification of the steel surface. The electrochemical and transport properties, as well as the thermal stability of epoxy coatings electrodeposited on steel and steel modified by Zn–Ni alloy were investigated during exposure to 3% aqueous NaCl.

3.4. *Electrochemical properties of the epoxy coating*

From the impedance plots in the complex plane for epoxy deposits formed on steel and steel modified by Zn–Ni alloy, the pore resistance, R_p, coating capacitance, C_c, and relative permitivity, ε_r, of the epoxy coating were obtained. The fitting of experimental data obtained from EIS measurements was accomplished using the equivalent electrical circuit given in Figure 5 and the fitting procedure elaborated by Boukamp [14]. The pore resistance and coating capacitance are plotted as a function of time of immersion in a 3% aqueous NaCl solution and are shown in Figures 6 and 7, respectively. The relative permittivity of the epoxy

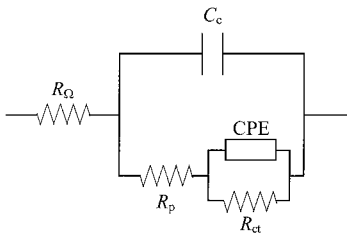

Fig. 5. Equivalent electrical circuit of a polymer-coated metal.

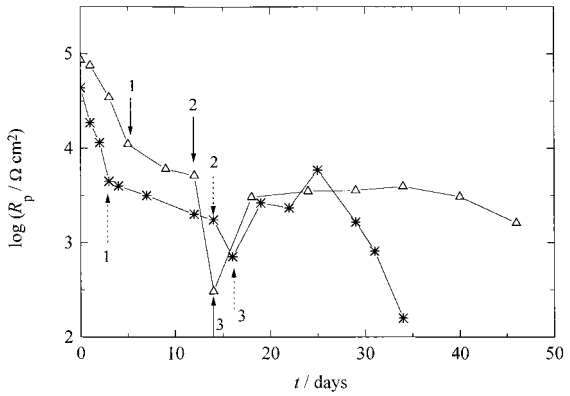

Fig. 6. Time dependence of pore resistance for epoxy coatings electrodeposited on steel (✱) and steel modified by Zn–Ni alloy (△) during exposure to 3% NaCl.

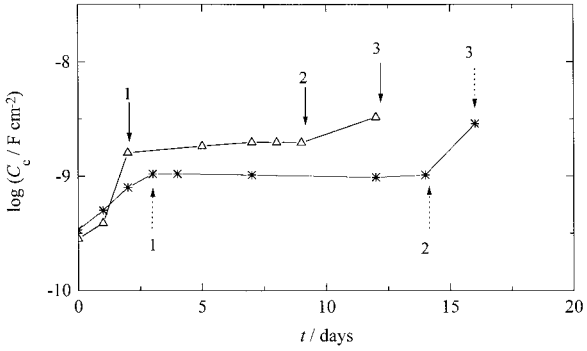

Fig. 7. Time dependence of coating capacitance for epoxy coatings electrodeposited on steel (✱) and steel modified by Zn–Ni alloy (△) during exposure to 3% NaCl.

coating, ε_r, was calculated from the film thickness, δ, and the coating capacitance using the equation:

$$\varepsilon_r = \frac{C_c \delta}{\varepsilon_0}$$

where $\varepsilon_0 = 8.85 \times 10^{-12}$ F m^{-1} is the permittivity of the vacuum. The time dependence of the relative permittivity is presented in Figure 8.

Initially, during the first three days for both samples, the pore resistance decreases (Figure 6, period up to point 1), while the coating capacitance (Figure 7) and the relative permitivitty (Figure 8) both increase with time, denoting entry of the electrolyte into the epoxy coating [10, 16, 17]. This is the first step of electrolyte penetration through an organic coating and it is related to water uptake, when molecules of pure water diffuse into the micropores of the polymer network according to Fick's law [18]. After this period, the values of the pore resistance, coating capacitance and relative permitivitty reach a plateau and remain almost constant over a longer period of time (Figures 6–8, period 1–2). This period of almost unchanged values of R_p and C_c characterizes the maintenance of the good protective properties of epoxy coatings [19]. This is the second step of electrolyte penetration and refers to the penetration of water and ions through the macropores of the coating. The

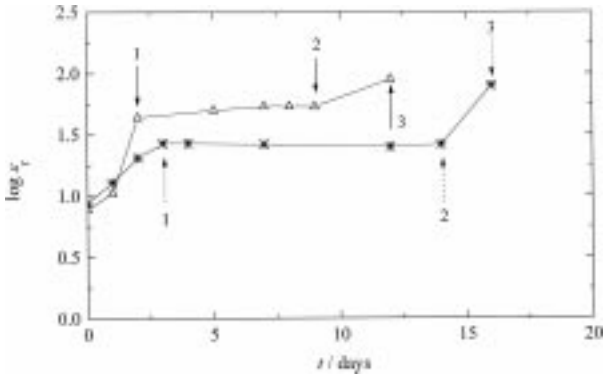

Fig. 8. Time dependence of relative permitivitty for epoxy coatings electrodeposited on steel (✱) and steel modified by Zn–Ni alloy (△) during exposure to 3% NaCl.

macropores become deeper with time, until they finally pass through the epoxy coating and reach the metal surface [20]. This leads to the beginning of electrochemical processes on the metallic interface, and, as a consequence, to the loss of adhesion. This detachment of the coating is characterized by an increase in capacitance of the coating (Figure 7, point 3) and a decrease in pore resistance (Figure 6, point 3) after a longer time of almost constant values. Although in the case of epoxy coatings on steel, the commencement of the corrosion reactions on the base substrate occurred a little later than on the Zn–Ni alloy, it can be concluded that the type of substrate does not significantly effect the electrochemical properties of epoxy coatings in this time interval. The profound influence of the surface modification is expressed during prolonged exposure to 3% aqueous NaCl (Figure 6, period after point 3).

The following period of increase and then decrease in pore resistance (Figure 6, period after point 3) for epoxy coating on steel can be explained by a plugging of the pores with corrosion products on steel during extended time of exposure, followed by further dissolution or desorption of the corrosion products [17]. On the other hand, the almost unchanged values of the pore resistance for epoxy coating on Zn–Ni alloy during a long time of exposure (Figure 6, period after point 3) indicate the great stability of this protective system due to existence of a passive layer on the Zn–Ni surface. It was shown [1, 21] that the passive layer on Zn–Ni surfaces in almost neutral chloride solution consists of basic salts, mainly $ZnCl_2 \cdot 4Zn(OH)_2$. So, the constant values of the pore resistance during extended time of exposure, can be explained by the plugging of the epoxy coating pores with corrosion products. These results point to a decreased corrosion rate on a steel modified by Zn–Ni alloy and that the passive layer of corrosion products is good barrier to the transport of water, oxygen and electrolyte ions.

The time dependence of the charge-transport resistance, R_{ct} (Figure 9) also confirms this behaviour. The initial decrease of R_{ct} on Zn–Ni alloy corresponds to the time required for the electrolyte to reach the metal surface and start the electrochemical process on the substrate. The further increase in R_{ct} corresponds to the

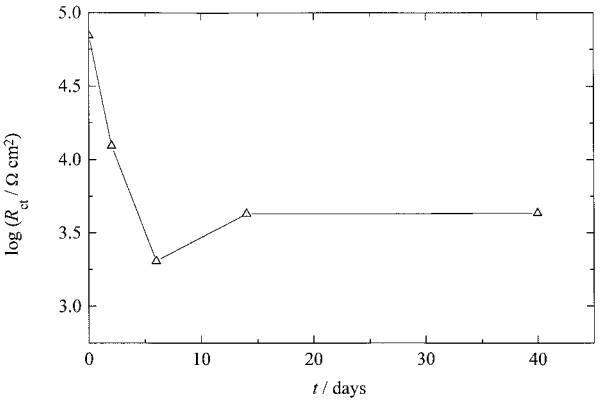

Fig. 9. Time dependence of charge transfer resistance for epoxy coating electrodeposited on steel modified by Zn–Ni alloy (△) during exposure to 3% NaCl.

increase in R_p, while the almost unchanged values of R_{ct} during the prolonged exposure again indicate good corrosion protection, due to the existence of a passive layer on the Zn–Ni surface.

3.5. *Transport properties*

The influence of steel surface modification on the sorption characteristics of epoxy coatings (first step of electrolyte penetration) was investigated by gravimetric liquid sorption experiments [18]. The reduced sorption curves (Figure 10) are plotted as dependence of m_t/m_∞ against $t^{1/2}/\delta$, since the second fickian diffusion law, for a flat plane and short times [22] is

$$\frac{m_t}{m_\infty} = \frac{4D^{1/2}}{\delta\pi^{1/2}} t^{1/2}$$

where m_t is the amount of absorbed water at time t, m_∞ is the amount of absorbed water in equilibrium, D is the diffusion coefficient of water through an epoxy coating and δ is the film thickness. As can be seen from Figure 10, the initial absorption of water is linear until a steady state is achieved. The initial linear region on the reduced sorption curves confirms the assumption that sorption is controlled by fickian diffusion. The diffusion coefficient of water through the epoxy coating is calculated from the slope of the initial region of the reduced sorption curves, and for an epoxy coating on steel it is 1.8×10^{-10} cm s^{-1}, and for an epoxy coating on steel modified by Zn–Ni alloy it is 7.2×10^{-10} cm s^{-1}. The lower value of D for the epoxy coating electrodeposited on steel than on modified steel indicates that the epoxy coating on steel has a less porous structure.

On the basis of the results obtained by EIS and gravimetric liquid sorption measurements, it can be concluded that the properties of epoxy coatings are strongly influenced by the surface on which they are electrodeposited. The different epoxy coating structure formed on different substrates can be explained by the rate of hydrogen evolution from steel and Zn–Ni alloy surfaces during the cathodic epoxy deposition, since hydrogen evolution by H_2O discharge is the first step in epoxy deposition [23], as well as by the difference in surface tension of the polymer solution on different substrates. Hydrogen evolves from a polymer solution on both the investigated surfaces at almost the same rate (Figure 11) but, the contact angle (measured by the drop test) between the polymer solution and the Zn–Ni alloy surface (35°) is greater than the contact angle on steel (29°). This indicates that the steel surface is better wettable than the Zn–Ni alloy. The larger contact angle on the Zn–Ni alloy than on the steel surface, although the rate of H_2 evolution is the same, causes an accumulation of H_2 on the cathode during electrodeposition of epoxy film, and, as a consequence, a more porous epoxy structure is formed on the Zn–Ni alloy. During the subsequent curing at 180 °C of the epoxy film, the H_2 is driven out leaving more vacancies in the polymer network and causing the epoxy coating on the Zn–Ni alloy to have a more porous structure [24] (greater $D(H_2O)$) in regard to epoxy coating on steel).

3.6. *Thermal stability of epoxy coating*

Thermal stability is a description of the chemical stability of a polymer at high temperatures, since

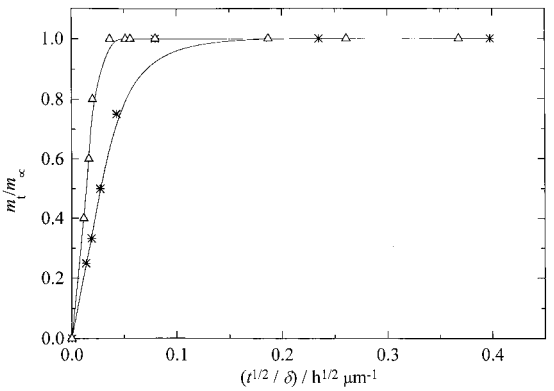

Fig. 10. Reduced sorption curves, at 25 °C, for epoxy coatings electrodeposited on steel (✱) and steel modified by Zn–Ni alloy (△) during exposure to 3% NaCl.

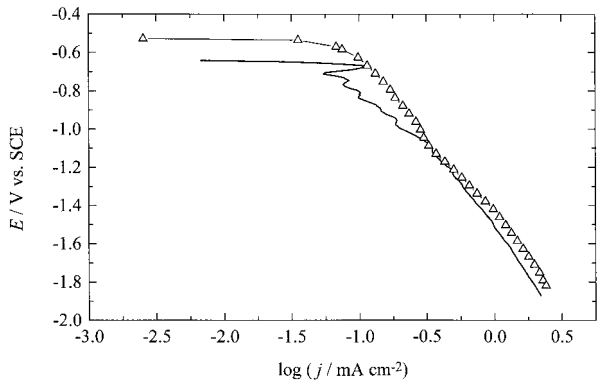

Fig. 11. Polarization curves for H_2 evolution on steel (—) and steel modified by Zn–Ni alloy (△), in a polymer solution at 25 °C, N_2 saturated, v = 0.5 mV s^{-1}, ω = 2000 rpm.

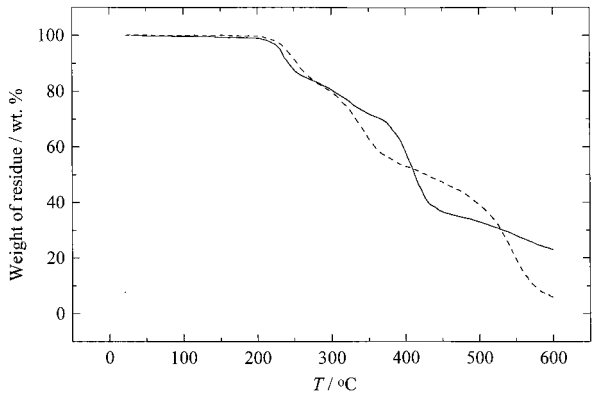

Fig. 12. TG curves for determination of thermal stability for epoxy coatings electrodeposited on steel (——) and steel modified by Zn–Ni alloy (- - - - -), after one day of exposure to 3% NaCl (heating rate 10 °C).

chemical processes that occur at elevated temperatures result in thermal degradation or crosslinking of high polymers. A qualitative characterization of the degradation process is, among other values, illustrated by the integral procedure decomposition temperature (*ipdt*), or the temperature corresponding to a 50% weight loss as an indication of the rate of thermal degradation [25].

The thermal stability of the epoxy coatings electrodeposited on both surfaces was investigated by TGA, after 1 day of exposure to 3% NaCl. The difference in the degradation temperatures of epoxy coatings on steel [26] and steel modified by Zn–Ni alloy [27] is shown in Figure 12. As can be seen, the *ipdt* value is greater for the epoxy coating on the Zn–Ni alloy (429 °C) compared to that for the coating on steel (413 °C). The different thermal properties are a consequence of the accumulation of H_2 during electrodeposition of the coating, as described earlier. It can be proposed, as a hypothesis, that the larger amount of accumulated hydrogen on the Zn–Ni alloy surface reacts with oxygen in the polymer chains causing an increased number of hydrogen bonds, and, consequently, the larger *ipdt* value for the epoxy coating on the Zn–Ni alloy. Hence, a more porous coating is formed on the Zn–Ni alloy, thus $D(H_2O)$ is greater and thermal stability is increased.

4. Conclusion

A Zn–Ni alloy with the best corrosion properties is obtained from chloride solution by deposition at 20 mA cm^{-2}. It was also shown that steel surface modification with this Zn–Ni alloy improves the corrosion stability of a protective system based on an epoxy coating, compared to an epoxy coating on steel.

During the initial time of exposure to 3% aqueous NaCl, the type of substrate effects the sorption characteristics and the thermal stability of the epoxy coating, but does not effect the electrochemical properties significantly.

The rate of hydrogen evolution during the electrodeposition of the epoxy coating is almost the same on both surfaces, but the smaller wettability of the Zn–Ni sublayer causes an accumulation of H_2 on the cathode which, during subsequent curing, exits, leaving more vacancies in the polymer network and resulting in the formation of a more porous epoxy coating on the Zn–Ni surface. As a consequence, the $D(H_2O)$ value of the epoxy coating on the Zn–Ni alloy is higher but the thermal stability is improved.

During prolonged exposure to a corrosive agent, the Zn–Ni alloy significantly improves the corrosion stability of the protective system: the R_p values remain constant over the entire investigated time, due to the formation of a passive layer of corrosion products which constitutes a good barrier to the transport of water, oxygen and electrolyte ions.

References

1. R. Fratesi, G. Lunazzi and G. Roventi, *in* L. Fedrizzi and P.L. Bonora (Eds), 'Organic and Inorganic Coatings for Corrosion Prevention' EFC Publication Vol. 20 (The Institute of Materials, London, 1997), pp. 130–143.
2. S.R. Rajagopalan, *Met. Finish.* **70** (1972) 52.
3. R. Fratesi and G. Roventi, *J. Appl. Electrochem.* **22** (1992) 657.
4. D.E. Hall, *Plat. Surf. Finish.* **70** (1983) 59.
5. M. Pushpavanam, S.R. Natarajan, K. Balakrishnan and L.R. Sharma, *J. Appl. Electrochem.* **21** (1991) 642.
6. W. Kantek, M. Sahre and W. Paatsch, *Electrochim. Acta* **39** (1994) 1151.
7. R.D. Srivastava and R.C. Mukerjee, *J. Appl. Electrochem.* **6** (1976) 321.
8. S. Swathirajan, *J. Electrochem. Soc.* **133** (1986) 671.
9. S. Swathirajan, *J. Electroanal. Chem.* **221** (1987) 211.
10. U. Rammelt and G. Reinhard, *Prog. Org. Coat.* **21** (1992) 205.
11. C. Karwas and T. Hepel, *J. Electrochem. Soc.* **135** (1988) 839.
12. V.B. Mišković-Stanković and M.D. Maksimović, *Prog. Org. Coat.* **18** (1990) 253.
13. B. Boukamp, *Solid State Ion.* **20** (1986) 31.
14. A. Brenner, 'Electrodeposition of Alloys', Vol. 1 and 2 (Academic Press, New York/London, 1963).
15. D.A. Porter and K.A. Easterling, 'Phase Transformations in Metals and Alloys' (Van Nostrand Reinhold, Wokingham, 1980).
16. G.W. Walter, *Corros. Sci.* **26** (1986) 27.
17. F. Deflorian, V.B. Mišković-Stanković, P.L. Bonora and L. Fedrizzi, *Corros. Sci.* **50** (1994) 438.
18. V.B. Mišković-Stanković, D.M. Dražić and Z. Kačarević-Popović, *Corros. Sci.* **38** (1996) 1513.
19. D.M. Dražić and V.B. Mišković-Stanković, *Prog. Org. Coat.* **18** (1990) 253.
20. V.B. Mišković-Stanković, D.M. Dražić and M.J. Teodorović, *Corros. Sci.* **37** (1995) 241.
21. M.R. Lambert, R.G. Hart and H.E. Townsend, SAE Tech. Pap. Series No 831817, Detroit, MI (1983) 81.
22. J. Crank, 'The Mathematics of Diffusion' (Clarendon Press, Oxford, 1970).
23. F. Beck, *in* J.O'M. Bockris, B.E. Conway, E. Yeager and R.E. White (Eds), 'Comprehensive Treatise of Electrochemistry', Vol. 2 (Plenum Press, New York, 1981), pp. 537–569.
24. V.B. Mišković-Stanković, M.D. Maksimović, Z. Kačarević-Popović and J.B. Zotović, *Prog. Org. Coat.* **33** (1998) 68.
25. V.V. Korshak, 'The Chemical Structure and Thermal Characteristics of Polymers' (Keter Press, Jerusalem, 1971).
26. V.B. Mišković-Stanković, J.B. Zotović, Z. Kačarević-Popović and M.D. Maksimović, *Electrochim. Acta* **44** (1999) 4269.
27. J.B. Zotović, Z. Kačarević-Popović, V.B. Mišković-Stanković and M.D. Maksimović, 50th ISE Meeting, Pavia, Italy (1999), Extended Abstracts Vol. 2, pp. 7–290.